THE JOURNAL OF PHYSICAL CHEMISTRY B

Article

pubs.acs.org/JPCB

Thin Layer-Based Spectral and Electrophoretic Study of Electro-Oxidation of Solid Ellagic Acid

Yu-Jiao Chen,[†] Ning Deng,[†] Bin Hu,[‡] Yan Wang,[†] and Jian-Bo He*[,†]

[†]Anhui Key Lab of Controllable Chemical Reaction & Material Chemical Engineering, School of Chemical Engineering, Hefei University of Technology, Hefei 230009, China

[‡]Anhui Sun-Create Electronics Co., Ltd., Hefei 230088, China

Supporting Information

ABSTRACT: Acquisition of data from both in situ spectroscopy detection and online chromatography-like separation is important for studying complex electrochemical reactions. The present work provides an example of combination of thin-layer spectral and electrophoretic electrochemistry, both based on thin-layer electrolysis. Two thin-layer electrochemical cells were used to investigate the electro-oxidation of solid ellagic acid at different potentials, in acidic, physiological, and alkaline buffer media. UV−vis spectra and cyclic voltabsorptograms of the oxidation products were recorded in situ without interference from the solid reactant. Four oxidation products, depending upon the buffer pH and the applied potential, were separated and detected by electrophoretic electrochemistry. The major products possess redox stability, possibly with a diquinonemethide structure. The minor product is considered as an *o*-quinone derivative with a lactone-ring-opening, which can be reduced or further oxidized at appropriate potentials. A consecutive-parallel reaction mechanism is proposed for the formation of four products of ellagic acid in different pH media, which enriches the knowledge about the oxidation pathway and antioxidant property of this biologically active polyphenol compound.

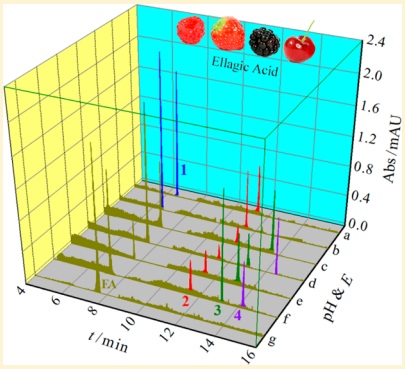

1. INTRODUCTION

Thin layer electrochemical cells, which contain an electrolyte solution usually in a microliter scale volume, can be used to realize almost 100% conversion of electroactive species in a short time. A typical example is the wide application of thin layer cells in spectroelectrochemistry, which allows an electrochemical reaction to be completed in several seconds to minutes and to be *in situ* monitored by various spectroscopic methods such as UV−vis,[1] ATR-FTIRS,[2] and SERS.[3] Electronic or vibrational spectroelectrochemistry can provide dynamic structural and/or electron transfer mechanistic information during oxidation or reduction of a molecule at an electrode surface. A new application of thin layer cells was developed in our group by coupling it with high-performance capillary electrophoresis (HPCE) and UV−vis detection.[4] This coupling method allows rapid exhaustive electrolysis, direct sampling, and online electrophoretic separation of the electrolysis products. In the present work, the spectral and electrophoretic measurements, both based on a thin layer cell, were performed to study the electro-oxidation of solid ellagic acid.

Ellagic acid (2,3,7,8-tetrahydroxy benzopyrano-5,4,3-cdebenzopyran-5,10-dione, abbreviated as EA) is a biologically active polyphenol compound found widely in fruits, vegetables, seeds, and some nuts in free form or in a bound state.[5,6] It is a natural antioxidant with the ability to scavenge superfluous superoxide free radicals,[7] and is usually used as an ingredient in cosmetic products for skin whitening.[8] Over the past few years, a number of in vivo and in vitro studies of EA have provided evidence of important pharmacological properties including anti-inflammatory,[9] anticoagulatory,[10] and anticarcinogenic activities.[11−13] It has been found that EA can extensively bind to protein and DNA, and their reversible binding to protein requires oxidation of EA by reactive oxygen species.[13]

The action of polyphenols as antioxidants has stimulated great interest on their oxidation and metabolism mechanisms.[14−18] The experiments of EA oxidation with mushroom tyrosinase indicated that the *o*-quinone was the first product of the enzyme action.[16] A product of EA with a diquinonemethide structure was also proposed to form during the conversion of Ag^+ ions to Ag nanoparticles.[19] Metabolism of EA in vivo was found to produce the dibenzopyranones known as urolithin A (3,8-dihydroxy-*6H*-dibenzopyran-6-one) and its monohydroxylated analogue known as urlithin B, which seems to be formed by lactone-ring cleavage, decarboxylation, and dehydroxylation reactions by the colon microbiota of different mammals.[17,20]

Because of the apparent parallelism between antioxidation and electro-oxidation, it is likely that the study of electro-oxidation of polyphenols could help, at least in part, in understanding their complex antioxidant mechanisms.[18] Simić et al. recently studied the electro-oxidation of EA in methanol aqueous media (1:1, v/v) within the pH range of 1.5−9.0, using cyclic voltammetry and by semiempirical calculations.[21] They

Received: September 30, 2013
Revised: January 30, 2014
Published: February 4, 2014

proposed an oxidation mechanism describing the formation of a semiquinone radical in various resonance forms and an *o*-quinone product in different deprotonated forms. Other electrochemical studies of EA oxidation mainly focused on the voltammetric determination of EA in various foodstuffs,[5] natural fruits,[6,22,23] and cosmetic products.[8] In addition, the electrochemical degradation of EA from aqueous solution was also studied using graphite and $RuO_2/IrO_2/TaO_2$-coated titanium electrodes.[24] It is generally considered that the initial electro-oxidation of EA is quasi-reversible, ascribed to a sequential formation of reactive phenoxyl radicals and then an *o*-quinone structure, while the second is irreversible, resulting from the formation of polymer film on the electrode surface. There is still considerable uncertainty about the oxidation pathway of EA, because it has multiple oxidizable −OH groups and two hydrolyzable lactone ring moieties.

The objective of this work is to obtain further information about the soluble products of EA oxidation in different pH media, by means of UV−vis transmission spectral analyses and capillary electrophoretic detection. One of the difficulties in studying EA is its poor solubility in water, especially in acidic aqueous media (pH < 5).[25,26] Therefore we studied EA oxidation by solid state electrochemistry, using a solid carbon paste electrode in which the EA microparticles were homogeneously dispersed in an accurately controlled amount. In this way, organic solvents were avoided, and the aqueous surrounding can be still kept. In addition, solid state spectroelectrochemistry can provide the time-dependent spectra of the resulting soluble products, free of the interference of insoluble reactants. The potential-dependent formation of the soluble products was also monitored in the present work by cyclic voltabsorptometry (CVA),[27,28] without the interference of EA.

2. EXPERIMENTAL METHODS

2.1. Chemicals and Solutions. Reagent-grade ellagic acid (98%+ pure) from HWRK Chem Co. (Beijing, China) was used as received. Spectrograde graphite powder (320 mesh) and spectrograde paraffin wax (solidification point 62−65 °C) from Shanghai Chemical Works were used for preparing the graphite paste electrode. Double-distilled water from an all-glass distillatory apparatus was used. Other chemicals were of analytical grade. Aqueous Britton-Robinson buffer solutions of 0.2 M containing 0.5 M KCl were adjusted to various pH levels as supporting electrolytes for electrochemical reactions. High pure N_2 was used to deaerate the electrolyte solutions. The background electrolyte (BGE) for capillary electrophoresis was a solution of 20 mM $Na_2B_4O_7$ at pH 9.3. The BGE additionally contained 20 mM sodium dodecyl sulfate (SDS) when used to re-equilibrate the capillary. All samples and solutions were filtered with a 0.45 μm nylon syringe filter (Shanghai Xingya purification materials Co., China) before injection.

2.2. Apparatus, Electrodes and Cells. All electrochemical measurements were conducted on CHI660C electrochemical workstation (Chenhua, Shanghai, China). UV−vis spectroscopic and photometric measurements were carried out on an UV-2500 spectrophotometer (Shimadzu, Japan) to monitor the soluble reactants and products under potentiostatic and potentiodynamic conditions. HPCE was measured on a CL1020 system (Cailu Scientific Inc., Beijing, China) equipped with a UV−vis detector (wavelength 190−740 nm). A bare fused-silica capillary with 50 μm I.D. and 400 μm O.D. (Yongnian Ruifeng Chromatoraphy Device, Hebei, China) was used as the separation channel.

The three-electrode system was composed of a solid EA-graphite-wax paste working electrode (EAGPE), an Ag/AgCl reference electrode, and a platinum wire counter electrode. The Ag/AgCl electrode contained a KCl saturated aqueous solution, and, except in the electrophoretic electrochemistry experiments, the Ag/AgCl wire was directly inserted to the electrolyte solution containing 0.5 M KCl. All the potentials reported in this paper are versus the potential of Ag/AgCl electrode with saturated KCl (0.197 V vs SHE). The EA-containing graphite paste was prepared by well blending EA powder with dried graphite powder and molten wax in a small beaker, and then was firmly pressed into the cavity of an electrode body before cooling/solidification. The ratio of graphite and wax was 5:2 (w/w), and the content of EA dispersed in the graphite paste was optimized as 6.5% (w/w). Unlike liquid-oil carbon paste, the surface of solid EAGPE can withstand polish on an emery paper and ultrasonic cleaning for about 10 s. The EAGPE used in a common cell was discal with a smaller geometrical area of 0.049 cm^2, whereas the EAGPE used in thin-layer cells was quadrate with a larger area of 0.80 cm^2. Carbon paste electrodes have advantages of low background currents, low noise, and fast baseline stabilization, and the fabrication was described previously.[29,30]

A common single-compartment cell was used for conventional voltammetric measurements. A thin-layer UV−vis spectroelectrochemical cell was self-made, using a standard quartz photometric cell with 10 mm optical path length as the cell body. A quadrate EAGPE with a PVC substrate was prepared as the working electrode (working area 0.80 cm^2). The incident light beam runs parallel to the working electrode and goes through the thin-layer electrolyte solution (10 mm long, 0.2 mm thick) on the electrode surface. A schematic view of the thin-layer spectral cell can be found in the literature.[28]

A thin-layer cell for electrophoretic electrochemistry was self-made on a single plastic chip, just 2.5 cm by 3.5 cm. The schematic view of the chip cell can be found in the literature.[4] It has a typical double layer structure consisting of a 1.5 mm-thick plastic coverslip on top of a 4 mm-thick plastic substrate. The centerpiece of the electrolysis part of the cell is a 1 cm^2 EAGPE electrode (working area 0.80 cm^2), which is held just above the plastic substrate by 0.2 mm-thick spacers, creating a thin-layer chamber under the electrode. The capillary then runs directly below this chamber, with a small hole in the bottom of the chamber, providing a way for any liquid injected into the chamber to pass into the capillary. After loading the sample, the open end of capillary is pushed to the inlet of a BGE reservoir for electrophoresis.

2.3. Procedures. At the beginning of each day, the thin-layer cells used were washed with double-distilled water and ethanol successively for 1 min under ultrasonication. The electrolyte solutions were bubbled with high pure N_2 for about 15 min to remove dissolved oxygen before put into the electrochemical cells. The working electrode was polished successively with 800 and 2000 grit emery papers. Between runs, the working electrode was cleaned by repetitive cyclic scans between 0.0 and 1.5 V vs Ag/AgCl in 0.1 M NaOH aqueous solution until only the background current presented. All the experiments were carried out at room temperature (22 ± 1 °C).

UV−vis absorption spectra were recorded repeatedly during potentiostatic electrolysis. The buffer supporting electrolytes

dx.doi.org/10.1021/jp4097259 | J. Phys. Chem. B 2014, 118, 2001−2008

were used for the spectral baseline correction. Multicycle cyclic voltabsorptometry was taken at a certain wavelength to follow the concentration changes of species in the thin layer solution.

The capillary had an effective length of 52 cm (from the inlet to the detector) and a total length of 60.5 cm. Before the electrophoresis experiments, the capillary was pressure-flushed sequentially with 1.0 M HCl for 5 min, double-distilled water for 5 min, 1.0 M NaOH for 10 min and double-distilled water again for 5 min. Finally, the capillary was re-equilibrated with the SDS-containing BGE for 10 min. For the first use, the EAGPE was polished with 800 grit emery papers, followed by ultrasonic cleaning in double-distilled water for 5 s. The SDS-free BGE was injected into the BGE reservoir within the thin-layer cell chip, and the electrolyte solution was injected into the thin-layer chamber. At a certain electrolysis time, the sample was hydrostatically sucked into the capillary at 20 cm height difference for a time of 20 s. The running voltage was 20 kV, and the detection wavelength was 253 nm. Between runs, the capillary was flushed with 0.1 M NaOH, double-distilled water, and the SDS-containing BGE each for 3 min. The detailed operating procedure related to the thin layer electrophoretic cell was described previously.[4]

3. RESULTS AND DISCUSSION

3.1. Cyclic Voltammetry. Figure 1 presents the CV curves of EAGPEs containing different amounts of EA, recorded in a common volume electrolytic cell. The pH value of the supporting electrolyte was equal to 1.8, close to stomach acid levels. A well-shaped anodic peak was observed at 0.77 V, with an extremely small cathodic counterpart at 0.60 V, indicating poor reversibility of EA oxidation. Accordingly, the major oxidation product of EA seems not to be the *o*-quinone derivative of EA, because *o*-quinone is electrochemically reducible.

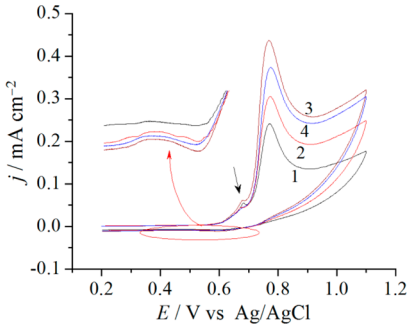

Figure 1. CV curves of EAGPEs in a common electrolytic cell. The content of EA in the graphite paste (wt%, 1→4): 3.5, 5.0, 6.5, 8.0; buffer pH 1.8; scan rate 50 mV s^{-1}. The inset is the enlargement of the cathodic branch.

The maximal oxidation current was obtained at an EA content of 6.5 wt % in the graphite paste, which therefore was selected in the following experiments. Just at the beginning of the main anodic peak occurred a very small anodic peak (indicated by a short arrow in Figure 1), which may be assigned to the oxidation of trace amount of EA dissolved from the solid EAGPE. For comparison, the CV curves of EA dissolved in aqueous-alcoholic solutions are provided in the Supporting Information (Figure S1). The oxidation of EA in free solution (pH 1.8, curve 1 in Figure S1) started at a less positive potential than that of solid EA (Figure 1), because a "break-in" overpotential is required for destroying the crystal structure of immobilized microparticles.[31] In addition, multiple anodic peaks can be distinguished for the EA dissolved in free solutions, corresponding to the successive oxidation of EA.

The anodic peak potentials ($E_{p,A}$) were found to shift negatively with increasing pH. A linear relationship, $E_{p,A}/V = 0.752-0.0570$ pH ($R = -0.9978$), was obtained for the anodic peak of solid EA. The value of Tafel slope indicates that an equal number of electrons and protons were involved in the oxidation of EA within the whole studied pH range. This result suggests that the initial oxidation of EA should occur at the phenolic hydroxyl groups to produce reactive phenoxyl radical species through one-electron one-proton transfer step. The extremely small cathodic peak shown in the inset of Figure 1 can be attributed to the reduction of the phenoxyl radical species. This unstable intermediate was more detected at the cathodic peak when the scan was reversed just after the anodic peak, especially at higher scan rates.

3.2. In Situ Thin-Layer Spectroelectrochemistry. Figure 2 shows the time-resolved UV–vis spectra of the thin-layer solutions (pH 1.8) recorded before and during the controlled potential oxidation of solid EA. The spectrum of 30 μM EA dissolved in a pH 1.8 aqueous-alcoholic solution is also present for comparison (the dashed curve in panel B). The EA in the solution has two major absorption peaks in the region 220–400

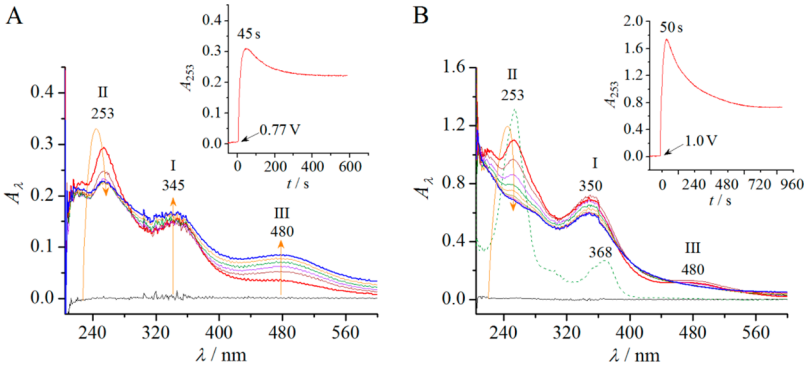

Figure 2. In situ thin layer UV–vis spectra of the oxidation products stripping from EAGPE with 6.5 wt % EA at a constant potential of 0.77 V (A) and 1.0 V (B). Buffer pH 1.8, time interval 79 s. The horizontal baselines in two panels were recorded before the potential was applied. The dashed curve in panel B is the UV–vis spectrum of 30 μM EA in pH 1.8 buffer solution containing 28 vt% ethanol. Insets: Chronoabsorptometric curves at 253 nm during oxidation at the corresponding potentials.

dx.doi.org/10.1021/jp4097259 | J. Phys. Chem. B 2014, 118, 2001–2008

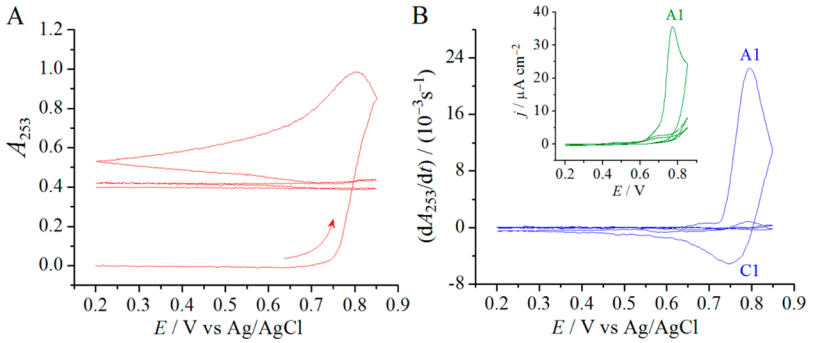

Figure 3. Multicycle thin-layer CVA (A) and DCVA (B) curves of EAGPE with 6.5 wt % EA in a potential range of 0.2−0.85 V. Buffer pH1.8, scan rate 2.0 mV s^{-1}, cycle number 3, wavelength 253 nm. Inset in panel B: the corresponding thin-layer CV curve.

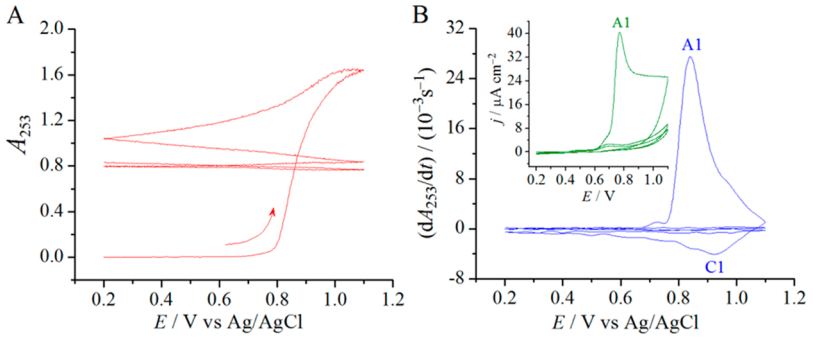

Figure 4. Multicycle thin-layer CVA (A) and DCVA (B) curves of EAGPE with 6.5 wt % EA in a potential range of 0.2−1.10 V. Buffer pH 1.8, scan rate 2.0 mV s^{-1}, cycle number 3, wavelength 253 nm. Inset in panel B: the corresponding thin-layer CV curve.

nm. These two peaks can be referred as band I (368 nm) and band II (253 nm) according to the nomenclature generally accepted for flavones.[32,33] The absorption in the band I region is generated by a $\pi-\pi$ transition from HOMO to LUMO orbitals. These orbitals are delocalized on the entire structure and this means that all the aromatic rings contribute to the transition, whereas the other frontier orbitals involved in the transition in the region II of the spectra are localized in specific rings.[32]

Before the potential was applied to the EAGPE, a horizontal spectral line was obtained, which proved the insolubility of EA in the pH 1.8 aqueous medium. During the oxidation of EA at 0.77 V (the anodic peak potential in Figure 1), three absorption bands appeared with maxima at 345 (band I), 253 (band II), and 480 nm (band III), respectively (Figure 2A). Oxidation at a more positive potential of 1.0 V resulted in a significant enhancement of the absorption in the regions of the bands I and II, and a slight red shift of the band I to about 350 nm (Figure 2B). The strong band II around 253 nm underwent an initial rise and subsequent fall in intensity, with a maximal absorption at an oxidation time of ca. 45−50 s (see the insets of Figure 2). This is a typical kinetics of an intermediate in successive reactions, e.g., phenoxyl radical species, which is generally formed during the oxidation of phenolic compounds. Between the bands I and II, no absorption bands were observed. This result can be used to exclude the possible formation of urolithin A and urolithin B.[17] The UV spectra of 20 bioavailable metabolites of ellagitannins and EA, including urolithins and nasutins, can be found in the literature.[33] Therefore, decarboxylation and dehydroxylation reactions seem not to occur during the oxidation of EA.

The weak and broad band III produced at both potentials is consistent with the result of EA oxidation by peroxynitrite, which led to a weak absorption in the 400−500 nm region.[7] The emergence of band III reflected a bathochromic effect, which suggests the occurrence of an extended conjugation system relative to that in the starting reactant. Some quinonoid compounds were observed to have weak absorption in this broad wavelength region.[34,35]

In the buffer solutions of pH 7.4 and 11.5 (>p$K_{a,1}$ of EA = 6.3),[16] EA underwent slight dissolution from the EAGPE to the solution, which interfered the spectral measurement of the oxidation products. For this reason, the spectroelectrochemical data were recorded for the EA dissolved in aqueous-alcoholic buffer solutions and are shown in the Supporting Information. At both pH values, the potentiostatic oxidation of EA led to a significant hypochromic effect in the regions of the bands I and II, accompanied by the emergence of the weak band III (Figures S2 and S3). The subsequent reduction at a cathodic potential partly recovered the absorption intensity in the bands I and II regions, but not including the band III. These results suggest that the oxidation of EA should yield at least one stable product that is electrochemically reducible, whereas the extended conjugation system responsible for the absorption at the band III is electrochemically irreducible.

3.3. Thin-Layer Cyclic Voltabsorptometry. Multicycle cyclic voltabsorptometry was performed in the thin-layer cell at the peak wavelength of the band II. Figure 3A shows the CVA curve of EAGPE in the pH 1.8 aqueous medium. During the cyclic scans, the variation of absorbance at 253 nm (A_{253}) reflects the formation and conversion of the soluble oxidation products of EA with potential. The first scan in the positive direction did not produce any light-absorbing substance in the thin-layer until the potential reached the region of the anodic peak, where the oxidation of EA resulted in a rapid increase in A_{253}. After the scan was reversed, the A_{253} continued to increase

dx.doi.org/10.1021/jp4097259 | J. Phys. Chem. B 2014, 118, 2001−2008

but soon started to fall back slowly to its steady-state value. In the subsequent cycles, the A_{253} nearly remained unchanged.

Figure 3B shows the time-derivative cyclic voltabsorptometry (DCVA) curve obtained by differentiating the CVA data in Figure 3A with time. A well-shaped DCVA peak A1 appeared at 0.796 V on the DCVA curve, corresponding to the anodic current peak at 0.772 V on the thin-layer CV curve (the inset of Figure 3B). After the scan was reversed, a cathodic counterpart C1 was seen only on the DCVA curve, which can be attributed to chemical conversion of an intermediate with absorption at 253 nm to a more stable product with less strong absorption at this wavelength. This intermediate is electrochemically stable in the potential region of peak C1, because no cathodic current peak occurred on the CV curve at the same time. The electroactive phenoxy radical intermediate also did not produce a cathodic current peak on the reverse scan. This result indicated that, at such a slow scan rate (2.0 mV s^{-1}), the phenoxy radicals were completely converted to the irreducible intermediate or other products before the scan was reversed. In the subsequent cycles, the anodic peak nearly disappeared from both the CV and DCVA curves, which indicated that the EAGPE surface was passivated after being subjected to the first redox cycling.

When the positive-going scan was extended to a more positive switching potential (1.10 V), the A_{253} continued to increase to higher levels with a trend to a limit value (Figure 4A). After the anodic peak on the CV and DCVA curves, the current signal still remained at a relatively high plateau, whereas the derivative absorbance signal decreased down to the baseline (Figure 4B). It can therefore be inferred that the dissolution of the oxidation products into the solution became increasingly difficult with increasing potential, because of their solubility limitation. In addition, the DCVA peak C1 appeared in a wide scan range of from 1.07 to 0.55 V (lasting for 260 s), with a peak potential higher than that of its anodic counterpart A1.This result further demonstrates that a slow chemical conversion should be responsible for the DCVA peak C1. It should be emphasized that the DCVA peak C1 could not be clearly detected for the EA in free solution due to the interference of the absorbance changes of EA.

The CVA and DCVA curves for the EA dissolved in pH 7.4 aqueous-alcoholic solution are shown in the Supporting Information (Figure S4). The wavelength was set at 264 nm, the peak wavelength of the band II at pH 7.4. The first scan in the positive direction first caused a slow decrease in A_{264} due to the potential-driven adsorption of EA, and then a fast decline in A_{264} due to the potential-driven oxidation of EA in the anodic peak region (Figure S4A). A minor peak pair C2/A2 was observed on both the CV and DCVA curves after the first positive scan (Figure S4B), with a midpoint potential more negative by ca. 0.27 V than the peak potential of the peak A1. Accordingly, the oxidation of EA yielded a stable product that can be electrochemically reduced at the peak C2. This minor product was most likely an *o*-quinone derivative of EA, as reported for EA oxidation with periodate, mushroom polyphenol oxidase, or platelet peroxidase.[16] This *o*-quinone derivative was reduced at peak C2 to the corresponding *o*-diphenol, which can be reversibly oxidized back to the *o*-quinone at the new anodic peak A2 (but not at the peak A1) in the next positive scan. It can therefore be deduced that, besides the *o*-diphenol groups, some other moiety of EA should have changed in the *o*-quinone derivative during the oxidation of EA. The redox peak pair C2/A2 cannot be observed at the EAGPE (Figures 3 and 4), because its surface was passivated after the first scan as mentioned above. The reason for the passivation occurring only in the case of solid EA needs further investigation.

In the subsequent cycles, the anodic peak A1 on both curves in Figure S4B showed a large decrease in intensity, due to the exhaustive and irreversible oxidation of EA in the thin-layer. Meanwhile, the peak pair C2/A2 remained stable in intensity, which is consistent with the good redox reversibility of *o*-diphenol/quinone couples.

3.4. Thin-Layer Electrophoretic Electrochemistry. The oxidation products of solid EA at three pH values were separated by HPCE/UV−vis method, based on the chip thin-layer electrolysis cell with a capillary channel and a BGE reservoir.[4] Figure 5 shows the electropherograms of 6.5 wt %

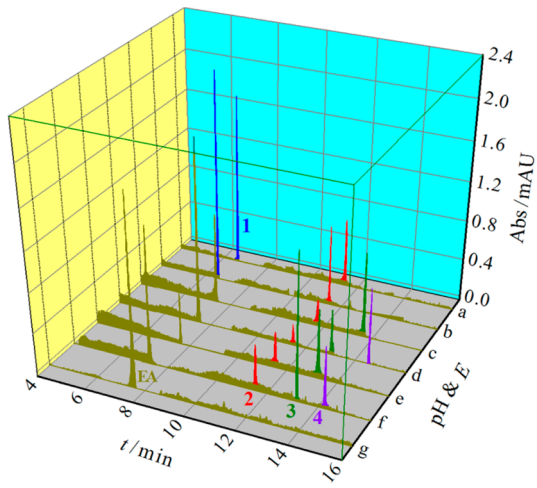

Figure 5. Electropherograms of 6.5 wt % EA in EAGPE after potentiostatic oxidation for 240 s. Electrolysis conditions: (a) pH = 1.8, E = 0.75 V; (b) pH = 1.8, E = 1.0 V; (c) pH = 7.4, E = 0.34 V; (d) pH = 7.4, E = 0.70 V; (e) pH = 11.5, E = 0.03 V; (f) pH = 11.5, E = 0.50 V; (g) pH = 11.5, open circuit. Electrophoresis conditions: BGE 20 mM $Na_2B_4O_7$ (pH 9.3), height difference 20 cm, sampling time 20 s, applied voltage 20 kV, detection wavelength 253 nm.

EA after potentiostatic oxidation for 240 s. At pH 1.8, only one negative peak occurred on the electropherogram recorded before electrolysis, with a migration time of ca. 4 min (data not shown). This peak can be assigned to a species involved in the buffer supporting electrolytes. No electrophoretic peak of EA was observed, demonstrating the insolubility of EA in the pH 1.8 aqueous solution. After oxidation at 0.75 or 1.0 V, two electrophoretic peaks appeared at ca. 6.4 and 11.3 min (curves a and b in Figure 5), respectively. Accordingly, two stable products (labeled as 1 and 2 in Figure 5) were formed at both the potentials.

At both the pH 7.4 and 11.5, a positive peak occurred on the electropherogram recorded before electrolysis, with a migration time of ca.7.5 min (e.g., curve g, labeled as EA). This peak can be assigned to the EA dissolving from the EAGPE into the solution. After electrolysis at a less positive potential, 0.34 V for pH 7.4 and 0.03 V for pH 11.5, two electrophoretic peaks appeared at ca. 11.3 and 13.2 min, respectively, besides the peak of the remaining EA (curves c and e). The product 2 and a new product 3 of EA were therefore detected. When the electrolysis was conducted at a more positive potential, 0.70 V for pH 7.4 and 0.50 V for pH 11.5, an additional peak was observed at ca. 14.3 min attributed to a new product 4 (curves d and f).

dx.doi.org/10.1021/jp4097259 | J. Phys. Chem. B 2014, 118, 2001−2008

The presence of acidic groups in an analyte may cause an increase in charge number and thus in the migration time of the analyte in the alkaline BGE. Product 1 has a migration time less than that of EA, supporting a conversion of phenolic hydroxyls to quinone but not to carboxyl. This product is the major product formed at pH 1.8, which has been considered, in the previous sections, to be electrochemically irreducible and have an extended conjugation structure (band III). Therefore, product 1 is likely to be the diquinonemethide derivative of EA, with a stable extended conjugation system. Similar diquinonemethides with electrochemical irreducibility have been reported as the oxidation products of some flavonols.[4,18,36,37] The formation of the diquinonemethide needs a chemical isomerization reaction following the electron transfer steps, as indicated by the presence of the DCVA peak C1 in Figures 3 and 4.

Product 2 corresponds to the minor product that may be an *o*-quinone derivative of EA with good redox reversibility. It has been deduced that, besides the phenolic hydroxyls, some other moiety in the *o*-quinone derivative should have changed during the oxidation of EA. With a migration time significantly longer than that of EA, the *o*-quinoid product 2 can be expected to contain a carboxyl group generated from the lactone-ring-opening.

Product 3 was formed at two higher pH values, 7.4 and 11.5, with the absence of product 1. The peak intensities of both products 1 and 3 were always significantly greater than that of product 2. Accordingly, product 3 formed in the alkaline media is likely to be a lactone-ring opened analog of the methide product 1. The lactone-ring-opening has been reported to occur during the metabolism of EA in vivo at the intestinal pH.[17,20] The resulting one or two carboxyl groups in product 3 made the migration time longer than that of product 1.

Product 4 was generated by the further oxidation of EA at the subsequent anodic peaks, in the pH 7.4 and 11.5 media (see CV curves 4 and 8 in Figure S1). Oxidation of EA by a strong oxidant may lead to oxidative disruption of a phenolic ring and then the formation of chebulic acid.[38,39] Therefore product 4 can be considered as chebulic acid, which contains three carboxyl groups and thus has the longest migration time.

On the basis of all the above observations and discussion, a consecutive-parallel reaction mechanism for the electro-oxidation of EA in acidic, physiological, and alkaline pH buffers is proposed and shown in Scheme 1. The phenoxyl radicals and then a disemiquinone intermediate were initially formed at the anodic peak A1 through two steps of one-electron one-proton oxidation. This intermediate was then converted to two types of products via isomerization and lactone-hydrolysis reactions: a diquinonemethide (product 1 or 3) and a lactone-ring opened *o*-quinone (product 2). This was a slow chemical transition lasting for several minutes under the thin-layer electrolysis conditions. Products 1 and 3, with good redox stability, were the major products formed in the acidic (pH 1.8) and the alkaline (pH 7.4 and 11.5) media, respectively. The product 2, with an *o*-quinone structure, can be reduced to the corresponding *o*-diphenol or further oxidized to chebulic acid (product 4), at the respectively required potentials.

Scheme 1. A Consecutive-Parallel Reaction Mechanism Proposed for the Formation of Four Electro-oxidation Products of EA in Different pH Media

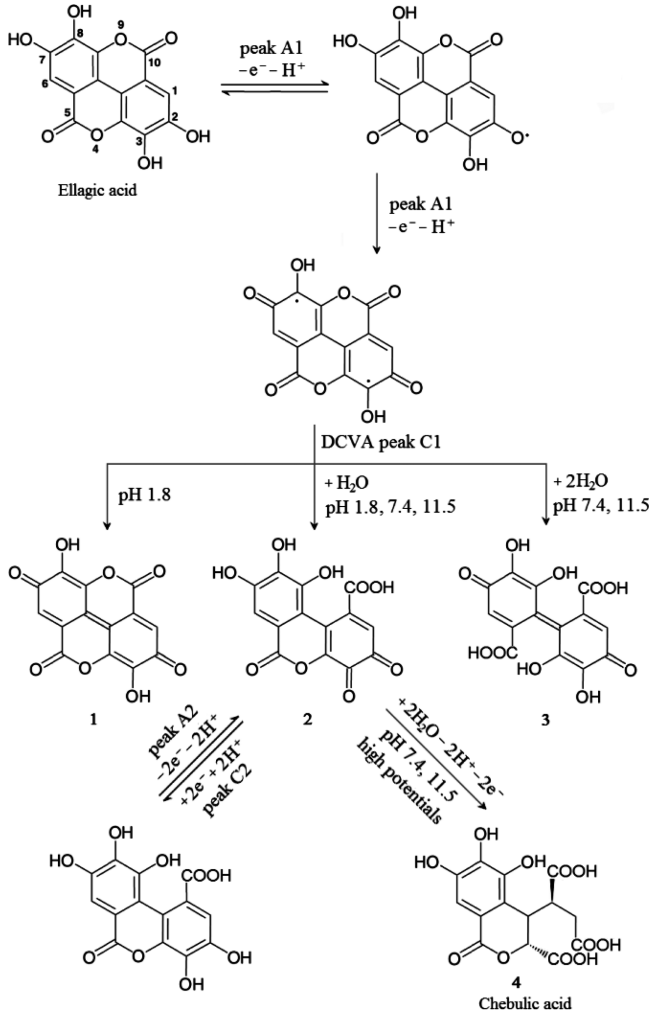

4. CONCLUSIONS

Electro-oxidation of ellagic acid is pH-dependent and four oxidation products were detected after its oxidation at different pH values and potentials. It was initially oxidized to reactive phenoxyl radicals and then to a disemiquinone intermediate via two steps of one-electron one-proton transfers. This intermediate may undergo isomerization and lactone-hydrolysis reactions leading to two types of products. The major products are different in the acidic and alkaline pH media, but both are possibly diquinonemethides with redox stability in the studied potential range. The minor product is considered as an *o*-quinone derivative with a lactone-ring-opening, which can be reduced or further oxidized at the appropriate potentials. This work provides an example of the combination of two methods both based on thin-layer electrochemical cells, and hence enriches the knowledge about the oxidation pathway and antioxidant property of ellagic acid.

■ ASSOCIATED CONTENT

Supporting Information

The CV, UV−vis, and CVA data of ellagic acid dissolved in free solution. This material is available free of charge via the Internet at http://pubs.acs.org.

■ AUTHOR INFORMATION

Corresponding Author

*E-mail: jbhe@hfut.edu.cn.

Notes

The authors declare no competing financial interest.

■ ACKNOWLEDGMENTS

We gratefully acknowledge the financial support from the National Nature Science Foundation of China (No. 21102030; 20972038) and the Research Fund for the Doctoral Program of Higher Education of China (No. 20130111110025).

■ REFERENCES

(1) Wang, Y.-H.; He, J.-B. Corrosion Inhibition of Copper by Sodium Phytate in Naoh Solution: Cyclic Voltabsorptometry for in Situ Monitoring of Soluble Corrosion Products. *Electrochim. Acta* **2012**, *66*, 45−51.

(2) Heinen, M.; Jusys, Z.; Behm, R. J. Ethanol, Acetaldehyde and Acetic Acid Adsorption/Electrooxidation on a Pt Thin Film Electrode under Continuous Electrolyte Flow: An in Situ ATR-FTIRS Flow Cell Study. *J. Phys. Chem. B* **2010**, *114*, 9850−9864.

(3) Godoi, D. R. M.; Chen, Y.; Zhu, H.; Scherson, D. Electrochemical Oxidation of Hydroxylamine on Gold in Aqueous Acidic Electrolytes: An in Situ SERS Investigation. *Langmuir* **2010**, *26*, 15711−15713.

(4) He, J.-B.; Cui, T.; Zhang, W.-W.; Deng, N. A Chip-Type Thin-Layer Electrochemical Cell Coupled with Capillary Electrophoresis for Online Separation of Electrode Reaction Products. *Anal. Chim. Acta* **2013**, *786*, 159−165.

(5) Cuartero, M.; Ortuño, J. A.; Truchado, P.; García, M. S.; Tomás-Barberán, F. A.; Albero, M. I. Voltammetric Behaviour and Square-Wave Voltammetric Determination of the Potent Antioxidant and Anticarcinogenic Agent Ellagic Acid in Foodstuffs. *Food Chem.* **2011**, *128*, 549−554.

(6) Ghoreishi, S. M.; Behpour, M.; Khayatkashani, M.; Motaghedifard, M. H. Simultaneous Determination of Ellagic and Gallic Acid in *Punica granatum*, *Myrtus communis* and Itriphal Formulation by an Electrochemical Sensor Based on a Carbon Paste Electrode Modified with Multi-Walled Carbon Nanotubes. *Anal. Methods* **2011**, *3*, 636−645.

(7) Priyadarsini, K. I.; Khopde, S. M.; Kumar, S. S.; Mohan, H. Free Radical Studies of Ellagic Acid, a Natural Phenolic Antioxidant. *J. Agric. Food Chem.* **2002**, *50*, 2200−2206.

(8) Chen, P.-Y.; Ji, Y.-M.; Luo, C.-H.; Chen, Y.-S.; Shih, Y. Quantification of Ellagic Acid in Cosmetic Products by Using a Partially Preanodized Screen-Printed Carbon Electrode Coupled with Flow Injection Analysis. *Anal. Methods* **2011**, *3*, 205.

(9) Rogerio, A. P.; Fontanari, C.; Borducchi, É.; Keller, A. C.; Russo, M.; Soares, E. G.; Albuquerque, D. A.; Faccioli, L. H. Anti-Inflammatory Effects of Lafoensia Pacari and Ellagic Acid in a Murine Model of Asthma. *Eur. J. Pharmacol.* **2008**, *580*, 262−270.

(10) Chao, P.-C.; Hsu, C.-C.; Yin, M.-C. Anti-Inflammatory and Anti-Coagulatory Activities of Caffeic Acid and Ellagic Acid in Cardiac Tissue of Diabetic Mice. *Nutr. Metab.* **2009**, *6*, 33.

(11) Weisburg, J. H.; Schuck, A. G.; Reiss, S. E.; Wolf, B. J.; Fertel, S. R.; Zuckerbraun, H. L.; Babich, H. Ellagic Acid, a Dietary Polyphenol, Selectively Cytotoxic to HSC-2 Oral Carcinoma Cells. *Anticancer Res.* **2013**, *33*, 1829−1836.

(12) Bell, C.; Hawthorne, S. Ellagic Acid, Pomegranate and Prostate Cancer—A Mini Review. *J. Pharm. Pharmacol.* **2008**, *60*, 139−144.

(13) Whitley, A. C.; Stoner, G. D.; Darby, M. V.; Walle, T. Intestinal Epithelial Cell Accumulation of the Cancer Preventive Polyphenol Ellagic Acid-Extensive Binding to Protein and DNA. *Biochem. Pharmacol.* **2003**, *66*, 907−915.

(14) Košinová, P.; Berka, K.; Wykes, M.; Otyepka, M.; Trouillas, P. Positioning of Antioxidant Quercetin and Its Metabolites in Lipid Bilayer Membranes: Implication for Their Lipid-Peroxidation Inhibition. *J. Phys. Chem. B* **2012**, *116*, 1309−1318.

(15) Galano, A.; León-Carmona, J. R.; Alvarez-Idaboy, J. R. Influence of the Environment on the Protective Effects of Guaiacol Derivatives against Oxidative Stress: Mechanisms, Kinetics, and Relative Antioxidant Activity. *J. Phys. Chem. B* **2012**, *116*, 7129−7137.

(16) Muñoz-Muñoz, J. L.; Garcia-Molina, F.; Garcia-Molina, M.; Tudela, J.; García-Cánovas, F.; Rodriguez-Lopez, J. N. Ellagic Acid: Characterization as Substrate of Polyphenol Oxidase. *IUBMB Life* **2009**, *61*, 171−177.

(17) Landete, J. Ellagitannins, Ellagic Acid and Their Derived Metabolites: A Review About Source, Metabolism, Functions and Health. *Food Res. Int.* **2011**, *44*, 1150−1160.

(18) He, J.-B.; Yuan, S.-J.; Du, J.-Q.; Hu, X.-R.; Wang, Y. Voltammetric and Spectral Characterization of Two Flavonols for Assay-Dependent Antioxidant Capacity. *Bioelectrochemistry* **2009**, *75*, 110−116.

(19) Kumar, K. M.; Sinha, M.; Mandal, B. K.; Ghosh, A. R.; Kumar, K. S.; Reddy, P. S. Green Synthesis of Silver Nanoparticles Using Terminalia Chebula Extract at Room Temperature and Their Antimicrobial Studies. *Spectrochim. Acta A* **2012**, *91*, 228−233.

(20) Sharma, M.; Li, L.; Celver, J.; Killian, C.; Kovoor, A.; Seeram, N. P. Effects of Fruit Ellagitannin Extracts, Ellagic Acid, and Their Colonic Metabolite, Urolithin A, on Wnt Signaling. *J. Agric. Food Chem.* **2010**, *58*, 3965−3969.

(21) Simić, A. Z.; Verbić, T. Ž.; Sentić, M. N.; Vojić, M. P.; Juranić, I. O.; Manojlović, D. D. Study of Ellagic Acid Electro-Oxidation Mechanism. *Monatsh. Chem.* **2013**, *144*, 121−128.

(22) Komorsky-Lovrić, Š.; Novak, I. Determination of Ellagic Acid in Strawberries, Raspberries and Blackberries by Square-Wave Voltammetry. *Int. J. Electrochem. Sci.* **2011**, *6*, 4638−4647.

(23) Komorsky-Lovrić, Š.; Novak, I. Abrasive Stripping Square-Wave Voltammetry of Blackberry, Raspberry, Strawberry, Pomegranate, and Sweet and Blue Potatoes. *J. Food Sci.* **2011**, *76*, C916−C920.

(24) Muthukumar, M.; Govindaraj, M.; Muthusamy, A.; Raju, G. B. Comparative Study of Electrocoagulation and Electrooxidation Processes for the Degradation of Ellagic Acid from Aqueous Solution. *Sep. Sci. Technol.* **2010**, *46*, 272−282.

(25) Queimada, A. J.; Mota, F. L.; Pinho, S. P.; Macedo, E. A. Solubilities of Biologically Active Phenolic Compounds: Measurements and Modeling. *J. Phys. Chem. B* **2009**, *113*, 3469−3476.

(26) Bala, I.; Bhardwaj, V.; Hariharan, S.; Kumar, M. N. V. R. Analytical Methods for Assay of Ellagic Acid and Its Solubility Studies. *J. Pharmaceut. Biomed.* **2006**, *40*, 206−210.

(27) He, J.-B.; Yu, C.-L.; Duan, T.-L.; Deng, N. In Situ Spectroelectrochemical Analysis of Quercetin in Acidic Medium. *Anal. Sci.* **2009**, *25*, 373−377.

(28) He, J.-B.; Wang, Y.; Deng, N.; Lin, X.-Q. Study of the Adsorption and Oxidation of Antioxidant Rutin by Cyclic Voltammetry−Voltabsorptometry. *Bioelectrochemistry* **2007**, *71*, 157−163.

(29) He, J.-B.; Ma, G.-H.; Chen, J.-C.; Yao, Y.; Wang, Y. Voltammetry and Spectroelectrochemistry of Solid Indigo Dispersed in Carbon Paste. *Electrochim. Acta* **2010**, *55*, 4845−4850.

(30) Hu, X.-R.; He, J.-B.; Wang, Y.; Zhu, Y.-W.; Tian, J.-J. Oxidative Spectroelectrochemistry of Two Representative Coumarins. *Electrochim. Acta* **2011**, *56*, 2919−2925.

(31) Scholz, F.; Schröder, U.; Gulaboski, R. *Electrochemistry of Immobilized Particles and Droplets*; Springer: Berlin, 2005.

(32) Mazzone, G.; Toscano, M.; Russo, N. Density Functional Predictions of Antioxidant Activity and UV Spectral Features of Nasutin a, Isonasutin, Ellagic Acid and One of Its Possible Derivatives. *J. Agric. Food Chem.* **2013**, *61*, 9650−9657.

(33) González-Barrio, R.; Truchado, P.; Ito, H.; Espín, J. C.; Tomás-Barberán, F. A. UV and MS Identification of Urolithins and Nasutins, the Bioavailable Metabolites of Ellagitannins and Ellagic Acid in Different Mammals. *J. Agric. Food Chem.* **2011**, *59*, 1152−1162.

(34) Mayer, J.; Krasiukianis, R. Absorption Spectra of the Radical Ions of Quinones: A Pulse Radiolysis Study. *J. Chem. Soc. Faraday Trans.* **1991**, *87*, 2943−2947.

(35) Chedekel, M. R.; Land, E. J.; Thompson, A.; Truscott, T. G. Early Steps in the Free Radical Polymerisation of 3,4-Dihydroxyphenylalanine (DOPA) into Malanin. *J. Chem. Soc., Chem. Commun.* **1984**, 1170−1172.

(36) Zhou, A.; Sadik, O. A. Comparative Analysis of Quercetin Oxidation by Electrochemical, Enzymatic, Air Oxidation, Enzymatic and Free-Radical Oxidation: A Mechanistic Study. *J. Agric. Food Chem.* **2008**, *56*, 12081−12091.
(37) Komorsky-Lovric, S.; Novak, I. Abrasive Stripping Voltammetry of Myricetin and Dihydromyricetin. *Electrochim. Acta* **2013**, *98*, 153−156.
(38) Haworth, R. D.; Pindred, H. K.; Jefferies, P. R. Chebulinic Acid. Part III. Oxidation of Ellagic and Flavellagic Acids and the Synthesis of Some Isocoumarin Derivatives. *J. Chem. Soc.* **1954**, 3617−3625.
(39) Haslam, E. Thoughts on Thearubigins. *Phytochemistry* **2003**, *64*, 61−73.